




SPK1/S1P axis confers gastrointestinal stromal tumors (GISTs) resistance of imatinib

Yan Chen^{1,2} · Rui Zhang² · Dandan Mi¹ · Qiuju Wang³ · Tingwenli Huang² · Xinwei Dong⁴ · Hongwei Zhang⁵ · Hongtao Xiao² · Sanjun Shi¹ 

Received: 20 June 2022 / Accepted: 8 August 2022

© The Author(s) under exclusive licence to The International Gastric Cancer Association and The Japanese Gastric Cancer Association 2022

Abstract

Background Imatinib mesylate (IM) is highly effective in the treatment of gastrointestinal stromal tumors (GISTs). However, the most of GISTs patients develop secondary drug resistance after 1–3 years of IM treatment. The aim of this study was to explore the IM-resistance mechanism via the multi-scope combined with plasma concentration of IM, genetic polymorphisms and plasma sensitive metabolites.

Methods This study included a total of 40 GISTs patients who had been regularly treated and not treated with IM. The plasma samples were divided into three experiments, containing therapeutic drug monitoring (TDM), OCT1 genetic polymorphisms and non-targeted metabolomics. According to the data of above three experiments, the IM-resistant cell line, GIST-T1/IMR cells, was constructed for verification the IM-resistance mechanism.

Results The results of non-targeted metabolomics analysis suggested that the sphingophospholipid metabolic pathway including the SPK1/S1P axis was inferred in IM-insensitive patients with GISTs. A GIST cell line (GIST-T1) was immediately induced as an IM resistance cell model (GIST-T1/IMR) and we found that blocking the signal pathway of SPK1/S1P in the GIST-T1/IMR could sensitize treatment of IM and reverse the IM-resistance.

Conclusions Our findings suggest that IM secondary resistance is associated with the elevation of S1P, and blockage the signaling pathway of SPK1/S1P warrants evaluation as a potential therapeutic strategy in IM-resistant GISTs.

✉ Sanjun Shi
shisanjuns@163.com; shisanjuns@cdutcm.edu.cn

¹ State Key Laboratory of Southwestern Chinese Medicine Resources, School of Pharmacy, Chengdu University of Traditional Chinese Medicine, No.1166 Liutai Avenue, Chengdu 611137, People's Republic of China

² Department of Clinical Pharmacy, School of Medicine, Sichuan Cancer Hospital and Institute, Sichuan Cancer Center, University of Electronic Science and Technology of China, Chengdu 610042, People's Republic of China

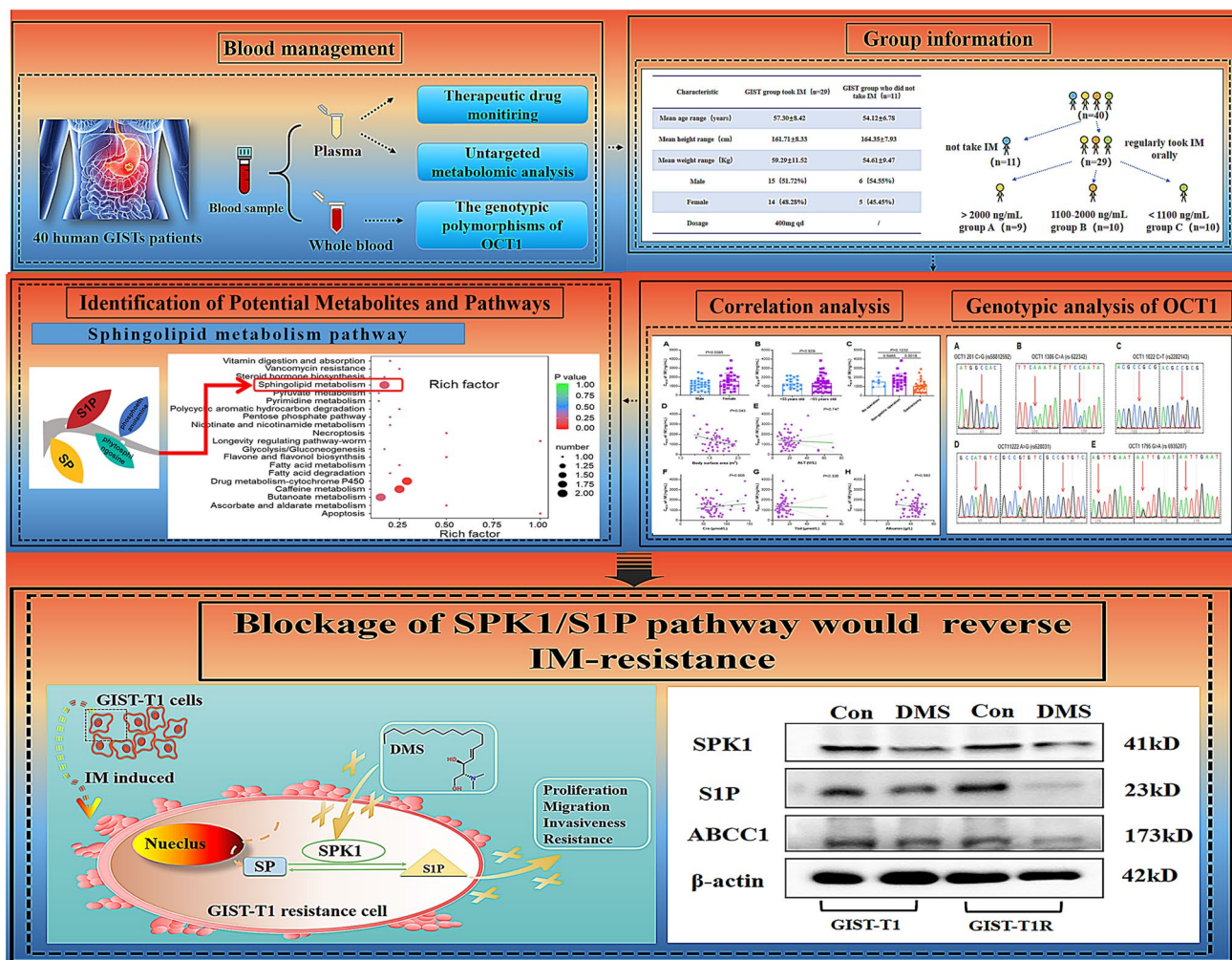
³ Department of Clinical Laboratory, School of Medicine, Sichuan Cancer Hospital and Institute, Sichuan Cancer Center, University of Electronic Science and Technology of China, Chengdu 610042, People's Republic of China

⁴ Department of Clinical Pharmacy, Nantong Tumor Hospital, Nantong 226300, People's Republic of China

⁵ Department of Anesthesiology, School of Medicine, Sichuan Cancer Hospital and Institute, Sichuan Cancer Center, University of Electronic Science and Technology of China, Chengdu 610042, People's Republic of China

Graphical abstract

The design of this study from blood management, group information collection, IM plasma concentration with different elements, identification of sphingolipid metabolism and lastly verification the function of SPK1/S1P in the IM-resistance GISTs cells.



Keywords Therapeutic drug monitoring · OCT1 genetic polymorphisms · Drug resistance · Sphingolipid metabolism · SPK1/S1P axis

Abbreviations

| | |
|---------|--|
| IM | Imatinib mesylate |
| GISTs | Gastrointestinal stromal tumors |
| TDM | Therapeutic drug monitoring |
| OCT1 | The role of organic cation transporter 1 |
| SNP | Single nuclear polymorphisms |
| PCA | Principal component analysis |
| OPLS-DA | Orthogonal partial least-squares discrimination analysis |
| KEGG | Kyoto encyclopedia of genes and genomes |
| FC | Fold-change |
| VIP | Variable importance for the projection |

| | |
|----------------|--|
| TKIs | Tyrosinase inhibitors |
| KIT | Tyrosine kinase |
| PDGFR α | Platelet-derived growth factor receptor α |
| CYP450 | Cytochrome P450 |
| OATP1 | Organic anion transporter protein 1 |
| NCCN | The National Comprehensive Cancer Network |
| ESI | Electrospray ionization |
| IQR | Interquartile range |
| PK | Pharmacokinetic |
| CER | Ceramide |
| SP | Sphingosine |

| | |
|------|-------------------------|
| S1P | Sphingosine-1-phosphate |
| Sm | Sphingomyelin |
| SPK1 | Sphingosine kinase-1 |

Background

Gastrointestinal stromal tumors (GISTs) are the most common mesenchymal tumors of the gastrointestinal tract and have the potential for malignant behaviors of recurrence and metastasis [1]. Surgical resection is the main treatment for GISTs [2], whereas oral targeted small-molecule drugs are mainly used for adjuvant therapy of GISTs with high recurrence and metastasis rates [3]. IM is a first-generation tyrosinase inhibitor (TKI) with remarkable success as an oral small-molecule targeted drug for first-line treatment of completely resected and high-risk GISTs as well as unresectable, relapsed and metastatic or advanced GISTs [4]. However, nearly 85% of GISTs patients develop secondary drug resistance after 1–3 years of IM treatment [5]. Thus far, mechanism analysis of IM resistance is very important, which has mainly focused on the following three aspects. (i) Acquired drug resistance caused by secondary mutations of receptor tyrosine kinase (KIT) or platelet-derived growth factor receptor (PDGFRA). As IM acts as an inhibitor targeting KIT and PDGFRA receptors, mutations in these two types of receptors would directly determine sensitivity to IM therapy [6, 7]. (ii) Some enzymes highly related with drug metabolism caused IM resistance. Because IM is mainly metabolized in the liver, with an oral bioavailability of 98%, polymorphisms in genes encoding liver metabolism enzymes, such as cytochrome P450 (CYP450) [8], and drug transport enzymes, such as P-glycoprotein ABCB1 [9], breast cancer resistance protein ABCG2 [10], organic cation transporter 1 (OCT1; SLC22A1) [11] and organic anion transporter protein 1 (OATP1; SLCO1A2) [12] can affect the IM concentration in serum. In general, secondary resistance to IM is related to a continuously insufficient serum concentration [4]. (iii) IM resistance may be attributed to activation of alternative survival pathways [13]. Herein, it is urgent and indispensable to realize the mechanism of IM resistance to ameliorate the long-term using of IM in clinic.

As an oral small-molecule targeted drug, IM exhibits huge intra-individual (approximately 75%) and inter-individual (60%) differences [14], and according to the National Comprehensive Cancer Network on the Diagnosis and Treatment of GISTs (NCCN, 2021 edition), determining the plasma drug concentration of IM after administration is of great clinical significance for patients with metastatic, relapsed and unresected GISTs [15]. At present, worldwide consensus is that a minimum concentration of IM should be above 1100 ng/mL [16]. When the concentration of IM in serum meets this standard, it is considered to be in effective

treatment. Meanwhile, as reported by our previous study, metabolism-correlated gene polymorphisms have a particularly significant influence on IM serum concentration [4].

Combined with research results on the mechanism of secondary drug resistance of IM, it has been speculated that the metabolic signaling pathway of IM might be related. Therefore, we grouped GISTs patients according to serum concentration of IM. After taken the same dosage of IM, the patients with high serum concentration of IM (> 2000 ng/mL) and middle serum concentration of IM (1100–2000 ng/mL) were considered as the sensitive IM treatment, while the patients with low serum concentration of IM (< 1100 ng/mL) were conducted as insensitivity to IM treatment. During IM treatment in clinic, IM resistance would not be totally mimicked only by serum concentration indeed. If the patients were identified as IM-resistance type, they would be rapidly given second or third generation of TKIs drugs, such as sunitinib [17] or regorafenib [18]. The use of sunitinib after IM resistance (5.5% objective response rate, median PFS 9.9 months) [19] and the use of regorafenib after sunitinib resistance (5.5% objective response rate, median PFS 4.8 months) [20] had limited ability to control the progression of GISTs in the clinical. Further in the latest year, avapritinib and ripretinib were approved by the FDA as novel TKIs. However, avapritinib was only approved for GISTs with PDGFRA mutations in exon 18, which benefits about 5% patients with GISTs [20]. Some patients with PDGFRA mutations treated within the recent phase I trial have progressed following an initial response to avapritinib [21]. According to a recent phase III trial data, the median PFS in the ripretinib group was only 6.3 months and the objective response rate was 9% [22]. Herein, it is urgently needed to explore the IM-resistant GISTs by focusing on the role of IM itself on the GISTs patients. Further, it would be a loss of IM-resistance-related study for that lack of IM serum samples. The serum concentration would be the most intuitive detection index reflected the sensitivity of IM *in vivo*, especially in the same dosage for a long time on the GISTs patients. To find the resistance germination based on serum concentration as soon as possible, therefore, in this study, the potential relationship between IM-insensitive type and serum significant metabolites were explored for the first time.

Herein, we performed a non-targeted metabolomics assay, which is broadly applied in metabolomic research and used to comprehensively and systematically analyse metabolites of all small molecular weights (< 1500 Da) [23]. The bioinformatic analysis would supply the potential significant pathway for IM treatment.

Meanwhile, gene polymorphisms of OCT1, which correlates with drug transportation in the liver [24], were examined. A member of the solute transporter superfamily [25], the OCT1 transporter is mainly expressed in the basolateral

membrane of hepatocytes and plays an important role in drug uptake into the liver. Its main function is to transport drugs into hepatocytes for metabolism or to pump drugs into intestinal epithelial cells [26]. The gene encoding the OCT1 transporter (SLC22A1) has significant polymorphisms [27]. OCT1 variants can cause partial loss of transporter function; this results in reduced or loss of transport efficiency and thus affects the blood concentration of IM as well as therapeutic efficacy, likely leading to drug resistance to IM caused by a continuously insufficient effective dose [28]. In view of this, combined with previous studies and polymorphism functional variability locus retrieval results, we selected OCT1 1759 G > A (rs 6935207), OCT1 201 C > G (rs 5812592), OCT1 1386 C > A (rs 622342), OCT1 1022 C > T (rs 2282143) and OCT11222 A > G (rs 628031) and studied their correlation with the IM plasma concentration in patients with GISTs to reveal subclinical markers of who taking IM and carrying OCT1 SNPs. The whole design of this study was supplied in Fig. 1.

2. Materials and methods

Ethical considerations

This study was conducted in accordance with the principles of the Declaration of Helsinki, and the study protocol was approved by the Research Ethics Committee of the Sichuan Cancer Hospital (Approval No. SCCHE-02-2020-044). Written informed consent was obtained from all individuals before participating in this study.

Study participants

Plasma samples were collected from 29 GISTs patients who took IM regularly with the dosage of 400 mg/qd and 11 GISTs patients who had never been taken IM from 2019 to 2021. The inclusion criteria for the GISTs group were as follows: (i) male or female aged ≥ 18 ; (ii) histopathological diagnosis of GISTs; (iii) continuous regular oral administration of IM 400 mg/d for more than 1 month, good compliance, no missed or less drug phenomenon. The exclusion criteria were as follows: (i) pregnancy or very poor mental or physical condition; (ii) taking IM and other targeted

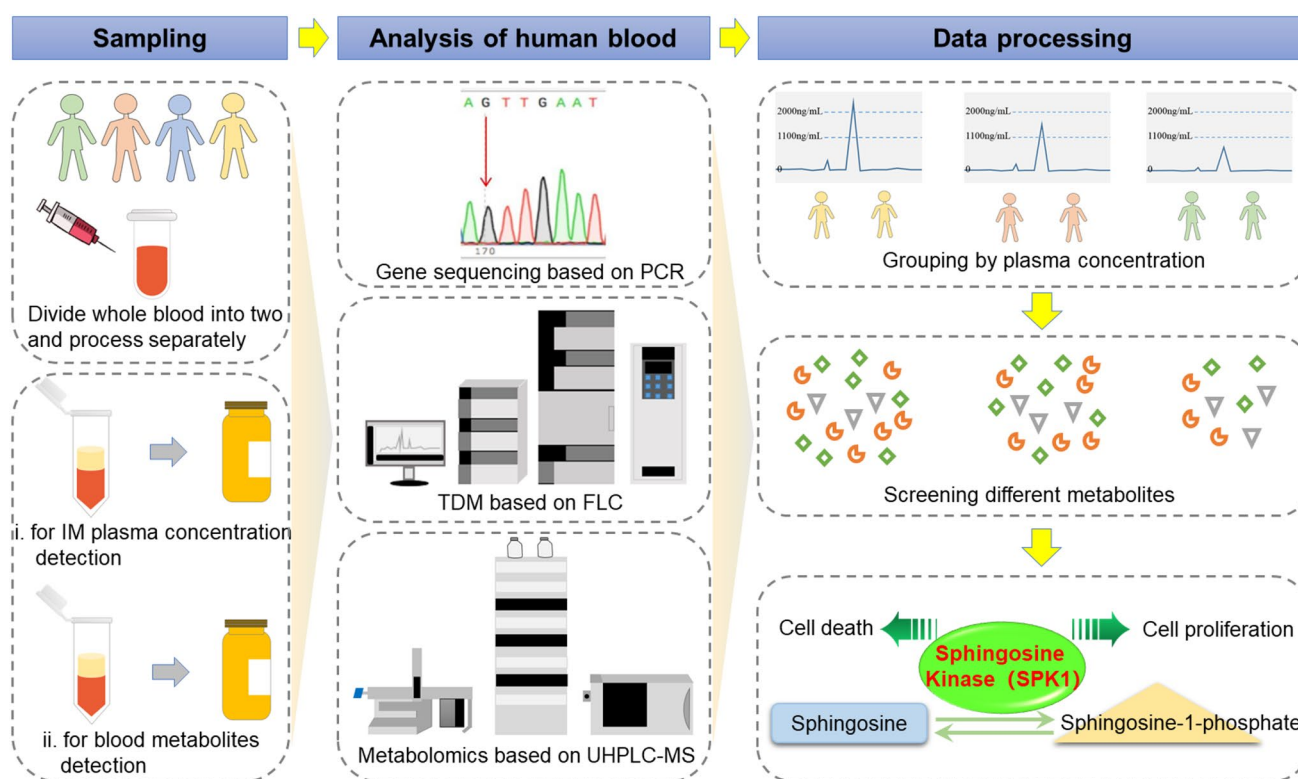


Fig. 1 The design of this study. Schematic illustration of process of samples based on different analysis assays, which were contained PCR, TDM of IM and sensitive metabolites screening of IM treat-

ment on GISTs patients. And the cell validation of IM-insensitivity was highly related with SPK1/S1P pathway. Blocking of SPK1/S1P pathway would confer the sensitivity of IM in GISTs therapy

drugs at the same time; (iii) organ failure or infection; (iv) poor compliance, with expected survival < 3 months; and (v) communication and cognitive impairment.

Plasma sample collection

The collection time of plasma sample was fixed to avoid the bad influence caused by different collection time point. Patients taking IM need to take the medicine regularly for more than 1 month to maintain a steady state of plasma concentration. Before blood collection, the patients were instructed to take IM at approximately 12:00, and blood was collected at approximately 10:00 the next morning. The collected peripheral venous blood was placed in an anticoagulation tube. At this time, the basic information of the patients was obtained, including name, sex, age and IM treatment. All samples were divided into a GISTs group (D) who had never been taken IM and a GISTs group (N) who took IM regularly. According to the results of IM plasma concentration, the GISTs group N was classified into 3 groups: an IM high-concentration group (A), an IM medium-concentration group (B) and an IM low-concentration group (C). For non-targeted metabolomics analysis, 1 mL of whole blood was taken from each sample and stored at -80°C ; multiple freeze–thaw cycles were avoided. The remaining whole blood was centrifuged at 5000 rpm for 5 min to obtain plasma, which was stored at -20°C until IM plasma concentration analysis.

Sample preparation and 2D-LC-UV instrument for TDM

The detail process was supplied in our previous study [29]. Briefly, plasma samples were injected directly to the system after the protein precipitation and centrifugation. Then they were detected by 2D-LC-UV instrument.

Pharmacogenetic analysis

Peripheral venous blood of patients was collected using a similar assay. Briefly, samples were added to cell lysate for interpretation, centrifugation and supernatant were removed. The precipitate was added with protease K, mixed, heated in water bath and then added with anhydrous ethanol, mixed and centrifuged. Repeated the above steps several times, added the eluent to the adsorption column, centrifuge and obtained the DNA. The five candidate SNPs [OCT1 1795 G > A (rs 6935207), OCT1 201 C > G (rs58812592), OCT1 1386 C > A (rs 622342), OCT1 1022 C > T (rs2282143), OCT11222 A > G (rs628031)] were analysed via first-generation gene sequencing. The primers used for each SNP were provided in Supplementary Data S1. The specific PCR process was as described in a previous report [30].

Sample preparation for untargeted metabolic profiling and operating condition

The plasma samples for untargeted metabolic profiling were detected by UHPLC-MS mass spectrometry with a 1290 Infinity LC ultrahigh-performance liquid chromatograph supplied by Agilent. The specific information was supplied in the Supplementary Data S2.

Cell culture and induction of IM-resistant cells

GIST-T1 cells, a constructed GIST cell line, were kindly supported by Ou's group [31] (Zhejiang Sci-Tech University, Hangzhou, China), which were cultured in RPMI 1640 (Gibco; Thermo Fisher Scientific, Inc., Waltham, MA, USA) medium containing 15% foetal bovine serum (TransGene Biotech, Beijing, China) and incubated at 37°C with 5% CO_2 . With a long term (8 months) and a continuously right dose impact administration of IM (from 10 to $50\ \mu\text{M}$), the IM-resistance GIST-T1/IMR cell line was successfully constructed.

Cell evaluation

For cellular morphological observation, the GIST-T1 and GIST-T1/IMR cells were displayed in the medium for the morphological observation under a light microscope from 10 to 40 amount of magnification. As indicated by previous report [32], cell growth curve and calculation of resistance index were carried out. Afterwards, to verify if SPK1 inhibitor *N,N*-dimethylsphingosine (DMS), could confer the sensitivity of IM treatment, these two cells were introduced onto the bottom of the 6-well culture plate with $5 \times 10^5/\text{mL}$ cells per well for cell scratch assay. After pretreatment of DMS ($10\ \mu\text{M}$) for 5 h, IM ($20\ \mu\text{M}$) was added to the cells for another 48 h. The medium was then replaced with complete medium containing 15% FBS. Cell invasion, colony formation, cell cycle and apoptosis analysis were also performed as usual described [33].

Western blot assay for detection of SPK1/S1P proteins

Western blotting analysis was performed as usually reported [34]. The GIST-T1 and GIST-T1/IMR cells were challenged with rabbit polyclonal anti-S1P (ab59870), anti-SPK1 (ab260073), anti- β -actin antibodies (ab8826) (Abcam company) and ABCC1 (DF7148) (Affinity company). Proteins were visualized with enhanced

chemiluminescence detection reagent according to the manufacturer's instructions (Pierce, Rockford, Illinois).

Data analysis

The pharmacogenetic data were analysed using SPSS 25.0 software. The Shapiro–Wilk method was used for testing of normality. Data that conformed to a normal distribution ($P > 0.05$) are represented by the mean (M) \pm standard deviation (SD), and an independent sample t test was used for comparisons between the two groups. Data not conforming to a normal distribution ($P < 0.05$) are represented by the median and interquartile range (IQR), and the Mann–Whitney U test was used for comparison between the two groups. The cut-off for statistical significance was set at $P < 0.05$ (two-sided). Fisher's exact probability method was employed to assess whether the frequency distribution of genotypes at each point comply with Hardy–Weinberg equilibrium.

The cellular data were statistically analysed using SPSS 20.0 software (IBM Corps., Chicago, IL, USA) and GraphPad Prism 6.0 (GraphPad Software, Inc.). The results are presented as the mean \pm standard deviation. Comparison of different groups was performed by one-way analysis of variance.

Results

Patient characteristics and groups

This study included 29 GISTs patients who regularly took IM orally and 11 GISTs patients who did not take IM (Supplementary data S3). The average ages of the GISTs patients with and without IM were 57.30 ± 8.42 and 54.12 ± 6.78 , respectively, with no significant difference. The groups also have similar heights, weights and sex ratios. The GISTs patients were divided into 4 groups according to whether they received IM treatment. Specifically, the first three groups (A, B and C) received 400 mg/qd of IM. Group A showed an IM plasma concentration > 2000 ng/mL ($n = 9$), Group B included an IM plasma concentration ranging from 2000 ng/mL to 1100 ng/mL ($n = 10$) and Group C contained an IM plasma concentration < 1100 ng/mL ($n = 10$). Group D ($n = 11$) was representative of IM missed patients. As shown in Supplementary data S4, the difference between the highest and lowest IM concentration was more than 12-fold, as reflected in the huge individual differences of GISTs patients under IM treatment.

Influencing factors of sex, age and surgical approach with mean plasma concentration of IM

According to our previous analysis [4], sex, age and operation should be important factors influencing the mean plasma

concentration of IM. In this study, we validated those factors as well. First, the plasma concentration of IM was detected, and the Shapiro–Wilk test for normality [35], Mann–Whitney U test for evaluating treatment effects of randomized elements [36] and independent t test for verifying statistically significant differences [37] were carried out to analyze related factors. The specific data between gender, age and surgical operation and C_{\min} of IM were shown in Supplementary data S5–S7. As depicted in Fig. 2A–C, the C_{\min} of IM in female patients was higher than that of male patients, which was in accordance with reports from the United Kingdom ($n = 93$) [38] and Switzerland ($n = 2478$) [39]. Potential factors are mean body weight and clearance rate. Long-term results from the United Kingdom [38] showed that when the plasma concentration of IM was normalized for body weight, differences in mean concentrations were no longer apparent. Thus, the higher plasma concentrations of IM in females may be partially explained by the lower body weight compared with males. Furthermore, the clearance rate of females was higher than that of males in the report from Switzerland [39]. Overall, the plasma concentration of IM was higher in the female group.

Age showed no significant difference in our study, which was different from Gotta et al. [39], who defined “young” as < 30 years of age and “elderly” as people up to 70 years of age. The young group exhibited low IM concentrations compared with the elderly group ($P < 0.05$). However, the median age in our study was 57.30 ± 8.42 . Specifically, the age of the included GISTs patients ranged from 40 to 78 years old, with no patients younger than 30 years old. Further, the sample of our study was limited due to COVID-19 [40]. As shown in Fig. 2C, the type of operation played an important role in the plasma concentration of IM, and the difference between the gastric surgery and non-gastric surgery groups was statistically significant. Similarly, Yoo et al. and Hompland et al. [41, 42] reported that C_{\min} was significantly lower in patients who had undergone major gastrectomy than in those who had undergone wedge gastric resection or did not undergo gastric surgery. Obviously, decreased absorption of IM might be caused in part by the lack of gastric acid secretion in GISTs patients who had undergone major gastric resection. Gastric acid secretion is extremely important for IM absorption because IM tablets dissolve rapidly at pH 5.5 or less [43].

Correlation among mean plasma concentration of IM_{\min} with body surface area and some essential serum index

Linear mixed model analyses can reveal similar trends, though sometimes without reaching statistical significance. A relationship between body surface area and the plasma concentration of IM was demonstrated in several reports [39,

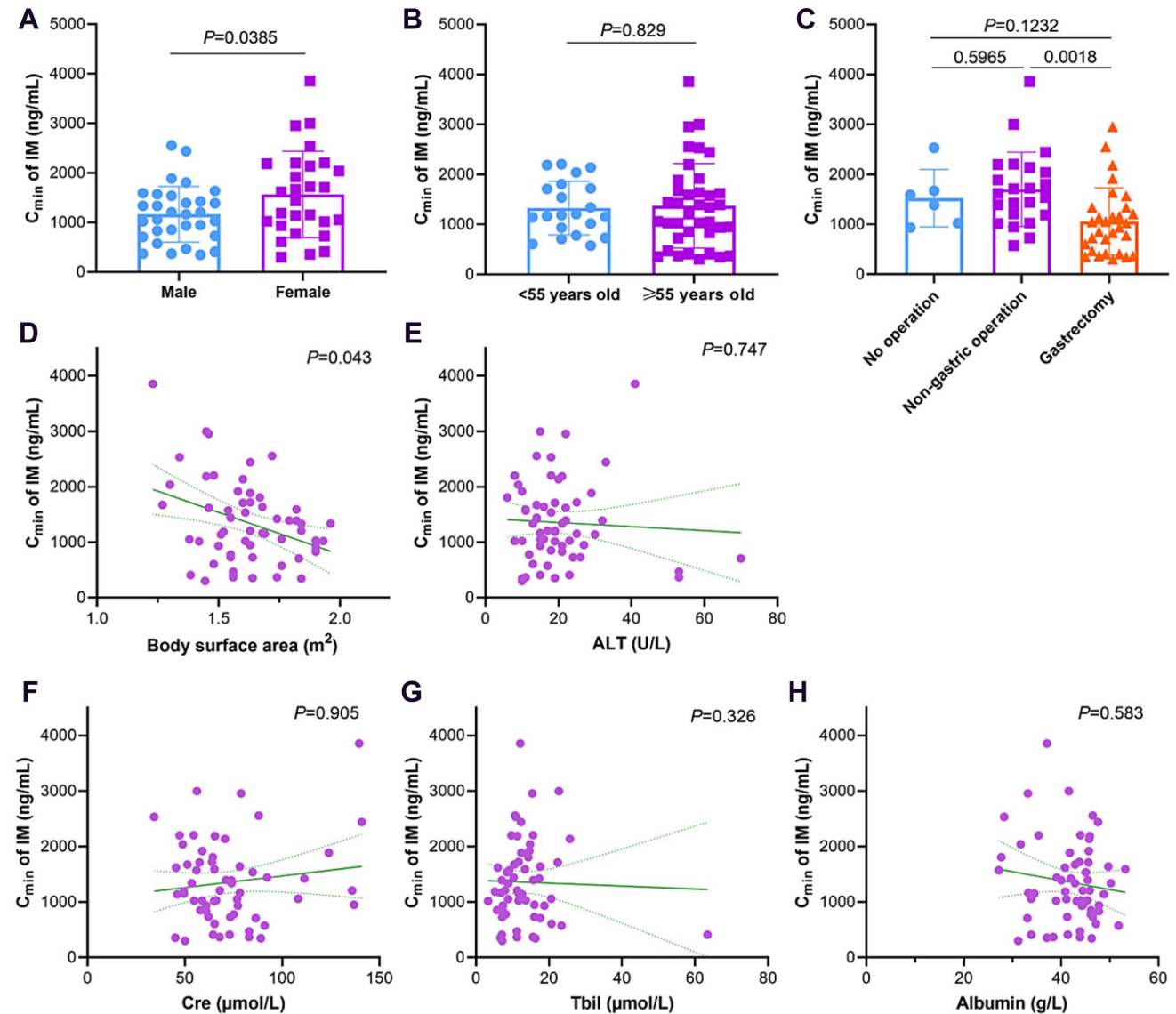


Fig. 2 Correlations between IM C_{min} and gender (A), primary surgical operation (B) and age (C). The linear mixed model analyses between IM C_{min} and body surface (D) and laboratory data of ALT

(E), creatinine (CRE) (F), total bilirubin (Tbil)(G) and albumin (H). $P < 0.05$ represents significantly difference

44]. As displayed in Fig. 2D, the body surface area exhibited a negative correlation with the IM plasma concentration ($P=0.043$). In other words, a higher dosage of IM should be given to patients with a smaller body surface area. It can be concluded from our results that a fixed dosage of IM might not be suitable for all of GISTs patients.

Laboratory data for ALT, creatinine (Cre), total bilirubin (Tbil) and albumin were also taken into consideration in this study. As illustrated in Fig. 2 E to H, there was no significant correlation between ALT ($P=0.747$), Cre ($P=0.905$), Tbil ($P=0.326$) and albumin ($P=0.583$) and the plasma concentration of IM. These findings for ALT was consistent with the report of Yoo et al. [41], though results for Cre and

Tbil were inconsistent with this report [44]. The reason may be associated with at least two factors. On the one hand, the number of GISTs patients in the abovementioned studies ranged from 25 to 89; the more eligible samples there are, the more reliable the statistics of the data are. However, the samples included in those studies were not sufficient. On the other hand, the influence of different ethnic populations should not be ignored. The association of albumin with C_{min} of IM is controversial. It has been suggested that more IM would be bound to albumin in patients with higher albumin, resulting in higher total C_{min} of IM according to Yoo [41], with albumin exhibiting a correlation with C_{min} of IM. However, the link between the albumin level and C_{min} of IM did

not reach statistical significance [42]. The actual relationship of albumin with the C_{\min} of IM plasma concentration is still unclear. Large-scale and multicenter trials of plasma concentrations of IM related to influencing factors need to be conducted, and the mechanism underlying the association should be explored, which would promote the rational use of IM in patients with GISTs.

Genotype of five OCT1 SNPs

Five SNPs (OCT1 1795 G>A (rs 6935207), OCT1 201 C>G (rs 58812592), OCT1 1386 C>A (rs 622342), OCT1 1022 C>T (rs 2282143), OCT11222 A>G (rs 628031)) in 29

patients were identified and the typing results are shown in Fig. 3A–E. The genotypes at OCT1 201C>G (rs 58812592) were all CC (wild-type). The other four candidate SNPs of OCT1 had mutations. The genotypic distribution of the four SNPs was summarized in Table 1. Only the remaining four SNPs were analysed by Hardy–Weinberg equilibrium, without showing deviation ($P>0.05$). Then, the relationship between genotypic SNPs and IM plasma concentration was assessed through the Mann–Whitney U test, as shown in Table 2. The two allelic locus at OCT1 1386C>A (rs 622342) were statistically significant ($P<0.05$) with IM plasma concentrations. The findings of 1022 C>T (rs 2282143) and 1222 A>G (rs 628031) were similar to those reported by Francis [45],

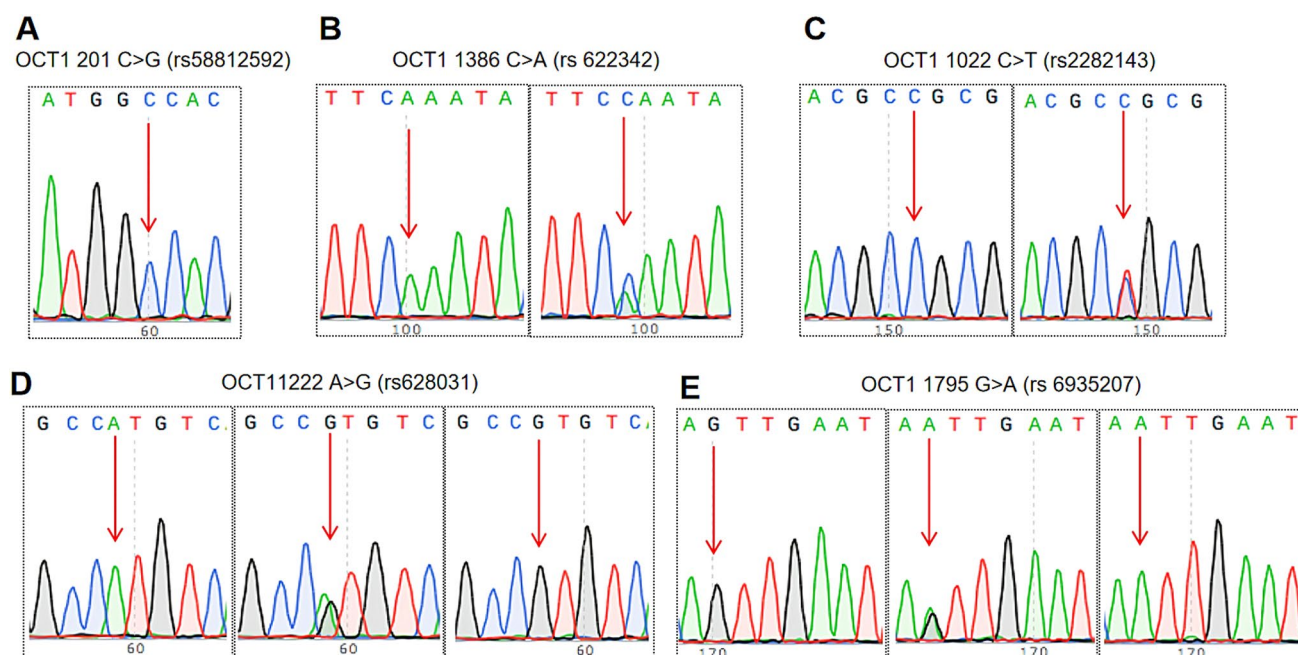


Fig. 3 The genotypic distribution of 5 SNPs on OCT1. A–E were displayed the locus of five OCT1, those were, OCT1 201C>G(rs58812592), OCT1 1386 C>A(rs622342), OCT1 1022

C>T(rs 2282143), OCT1 1222 A>G(rs 628031), OCT1 1795G>A (rs 6935207). The red arrows indicated mutation of the allele

Table 1 Genotype distribution of SNPs locus via Hardy–Weinberg equilibrium analysis

| SNPs | Gene type | Number | Genotype frequency (%) | Theoretical value | P_{H-W} |
|---------------------------|-----------|--------|------------------------|-------------------|-----------|
| OCT1 1022C>T (rs2282143) | CC | 22 | 75.86 | 22 | >0.05 |
| | TC | 7 | 24.14 | 6 | |
| OCT1 1386C>A (rs 622342) | AC | 5 | 17.24 | 5 | >0.05 |
| | AA | 24 | 82.76 | 24 | |
| OCT1 1222 A>G (rs 628031) | AA | 1 | 3.45 | 1 | >0.05 |
| | AG | 10 | 34.48 | 10 | |
| | GG | 18 | 62.07 | 18 | |
| OCT1 1795G>A (rs 6935207) | GG | 8 | 27.59 | 7 | >0.05 |
| | AG | 13 | 44.83 | 15 | |
| | AA | 8 | 27.59 | 7 | |

Table 2 Relationship between IM plasma concentration and 4 genotypic SNPs

| SNPs | Gene type | Number | Plasma concentration (ng mL ⁻¹) | <i>P</i> |
|------------------------------------|-----------|--------|---|----------|
| <i>OCT1</i> 1022C > T (rs 2282143) | CC | 22 | 1511.68 ± 842.38 | – |
| | TC | 7 | 1745.69 ± 1092.90 | |
| <i>OCT1</i> 1386C > A (rs 622342) | AC | 5 | 1488.81 ± 1375.69 | 0.005* |
| | AA | 24 | 1584.70 ± 800.84 | |
| <i>OCT1</i> 1222 A > G (rs628031) | AA | 1 | 300.34 | – |
| | AG | 10 | 1824.62 ± 1009.31 | |
| | GG | 18 | 1496.13 ± 798.24 | |
| <i>OCT1</i> 1795G > A (rs6935207) | GG | 8 | 1699.52 ± 890.48 | – |
| | AG | 13 | 1861.02 ± 978.17 | |
| | AA | 8 | 960.92 ± 400.60 | |

P values were calculated from Mann–Whitney *U* test

*Represents *P* < 0.05

who included 73 patients with IM-treated chronic myeloid leukaemia.

Multivariate statistical analysis of metabolites

PCA was performed as an unsupervised analysis. The advantage of PCA is that it reduces the number of highly correlating metabolic features to a smaller set of principal components. This superiority enables PCA score plots to provide a visual description of the pattern described by the model that can be used for the identification of batch effects [46]. The results of PCA are illustrated in Fig. 4A, B, G–F. In both 2D and 3D plots, the IM-treated groups (A, B and C) are distinguished from untreated Group D, no matter in the ESI⁺ or ESI⁻ mode. These results encouraged us to perform further statistical analysis.

The problem of insensitivity of variables with small correlation, which is a deficiency of PCA, may be overcome by the OPLS-DA model. We evaluated the reliability and predictive ability of the OPLS-DA model, and all of the parameters R^2X , R^2Y and Q^2 met the standard. When Q^2 was closer to 1, the model was more suitable and reliable [47]. Simultaneously, $Q^2 > 0.5$ is considered to be an effective model [48]. As shown in Fig. 4C–E, H–J, Q^2 among the three comparison groups, were always more than 0.8, which indicated that the models were all successful and that biochemical changes between groups were clear. Further, there was a clear separation between the IM-treated groups (A, B and C) and Group D. Concurrently, the samples from these groups tended to cluster in a concentrated manner, with a high degree of aggregation.

Identification of potential metabolites and pathways

Peaks were aligned, and missing values were eliminated from the UHPLC/MS data. 2238 and 1020 metabolites

in the ESI⁺ and ESI⁻ modes were screened through publicly available databases, respectively, which were demonstrated in Supplementary data S8.

Subsequently, different metabolites were selected using a fold-change threshold > 2 or < 0.5 , $VIP \geq 1$, and Student's *t* test threshold $P < 0.05$ [49, 50]. The significant metabolites were illustrated in Fig. 5A–C. The most abundant class of metabolites was lipids and lipid-like molecules, including D-sphingosine, 1-sphingosine phosphate, phytosphingosine and phosphoethanolamine. The *N*-desmethylimatinib was one of the major IM metabolites, which was also confirmed by this study.

The distribution and probability density of the top 20 differential samples in above mentioned groups were inspected by a violin box [51]. The thin black line extending from the violin box represents the 95% confidence interval, the black bar in the middle of the violin box represents the median value, and the outer shape represents the distribution density of the samples. As depicted in Supplementary data S9–S10, the differential metabolites in groups D to A, B and C exhibited different distribution patterns, which indicated the capacity to distinguish these metabolites in the groups treated or not with IM.

KEGG (<http://www.kegg.jp>) is not only an encyclopedia of genes and genomes but also a professional tool for metabolites and non-metabolic pathways [52]. Pathways are considered significantly enriched if $P < 0.05$, and the impact number of metabolite hits in the pathway is > 1 [53]. The greater the number of metabolite hits in the pathway with a lower *P* value, the greater pathway match. As displayed in Fig. 5D–F, the signaling pathways included sphingolipid metabolism, drug metabolism (CYP450), butanoate and caffeine metabolism, among others. Sphingolipid metabolism had the greatest commonness among the three groups, with impact numbers greater than 1.75 and value of *P* below 0.05.

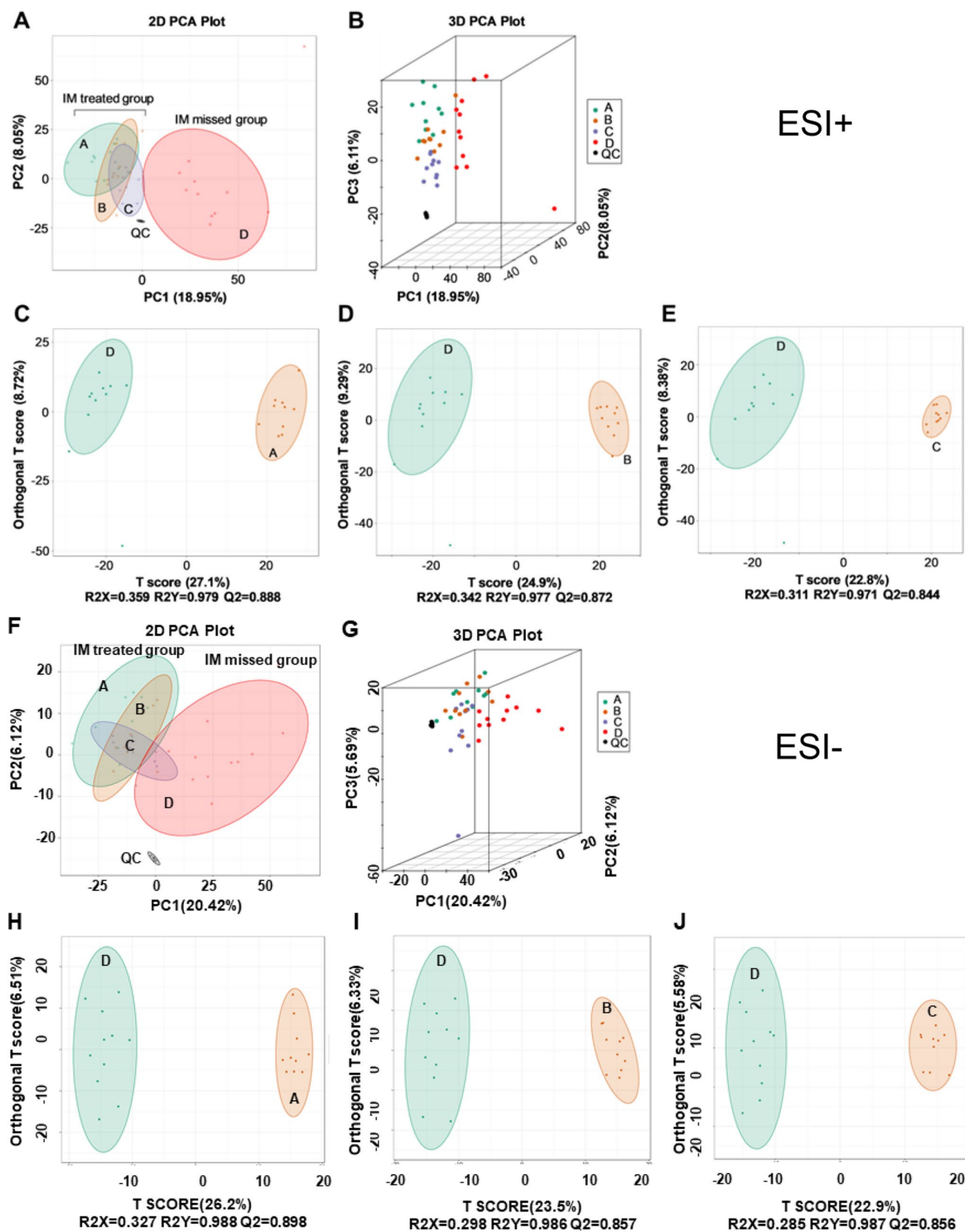


Fig. 4 Multivariate statistical analysis of metabolites. **A, B** 2D and 3D of PCA score plots of model groups (A, B and C) compared to group D in the mode of ESI^+ . The X axis represents the first principal component, the Y axis represents the second principal component and the Z axis represents the third principal component. The black mix represents the quality control (QC) sample during the detection process. **C–E**. OPLS-DA score plots of model groups (A, B and C) compared to group D, respectively, in the mode of ESI^+ . **F, G**. 2D and 3D of PCA score plots of model groups (A, B and C) compared to group D in the mode of ESI^- . **H, I**. OPLS-DA score plots of model groups (A, B and C) compared to group D, respectively, in the mode of ESI^-

In recent years, sphingolipid metabolism has been shown to play an important role in the proliferation, migration, inflammatory response and activation of various tumor cells [54]. Especially the sphingophospholipid metabolism, which belongs to sphingolipid metabolism, produces a variety of metabolites, such as ceramide (CER), sphingosine (SP), sphingosine-1-phosphate (S1P) and sphingomyelin (Sm) [55]. These above-mentioned molecules involved in the regulation of tumor proliferation, invasion and angiogenesis [55]. Studies have confirmed that CER and SP inhibit cell growth and promote apoptosis [56]; their further metabolite S1P inhibits apoptosis and promotes cell proliferation [57]. Therefore, the dynamic balance of CER/S1P determines whether tumor cells undergo apoptosis or proliferation. Sphingosine kinase-1 (SPK1) generates S1P by phosphorylating SP, a product of CER, and SPK1 is a key enzyme for S1P synthesis and CER/S1P homeostasis regulation [58]. Studies have shown that overexpression of SPK1 promotes expression of the PI3K/Akt signaling pathway in triple-negative breast cancer, thus enhancing the proliferation and metastasis of triple-negative breast cancer cells, which would be a potential mechanism of tumor drug resistance [59]. The combination of SPK1 and bortezomib can reverse the sensitivity of IM-resistant chronic myelogenous leukaemia (K562) cells by down-regulating Mcl-1 expression [60]. Herein, we speculated that the SPK1/S1P pathway would be involved in modulating IM-resistance GIST therapy. In the following study, we made IM-induced resistant GIST cells to verify the inner mechanism, which never been reported in the treatment of GISTs.

Establishment of the IM-resistant GIST-T1/IMR cell line

As reported by Ou's group [31], the GIST-T1 cells were imatinib-sensitive GIST cells, which could be recommended to simulate the treatment of IM in the first clinical therapy effect. Herein, over 8 months, the IM-induced resistant GIST-T1/IMR cell line was successfully constructed. As supplied in the Supplementary data S11, the IC_{50} value of GIST-T1/IMR cells was 39.24 μ M, while the value of GIST-T1 cells was 7.862 μ M. The drug resistance index (RI) was

nearly 5, suggesting that GIST-T1/IMR cells belonged to drug resistance cell line after long-term induction of IM [61]. DMS, belongs to one of effective sphingosine kinase inhibitors and verified high inhibitory activity on SPK1 compared to SPK2 [62]. To verify the role of SPK1/S1P in the IM-resistance GISTs cell line, we pretreated DMS to GIST-T1/IMR and GIST-T1 cells, respectively, to explore the change of IC_{50} from IM. The values in the DMS pretreatment group were decreased dramatically when compared to IM treatment only, which supplied in the Supplementary data S12. This phenomenon suggested IM related drug resistance was highly related with SPK1/S1P pathway.

GIST-T1 cells, a fiber cell form, were adherent to growth [63], which were displayed as fusiform or irregular triangle, and surrounded by length of spike usually. Increasing gradually with IM dose and exposure time, the GIST-T1 cells were illustrated as shrinkage of cell volume, increase of intercellular space, intracellular black granules and vacuoles. Further the boundary of cells was not clear, as depicted in Fig. 6A.

As displayed in Fig. 6B, E, scratch test results showed that GIST-T1 and GIST-T1/IMR cells had similar scratch healing rate at 24 h ($P > 0.05$). When cells treated with IM, the migration rate of GIST-T1/IMR was significantly higher than GIST-T1 ($P < 0.01$), suggesting GIST-T1/IMR had a certain tolerance ability to IM comparison with GIST-T1 cells. In addition, the scratch healing rate in the pretreatment with DMS groups significantly decreased compared with only IM treatment ($P < 0.01$), which illustrated that DMS could affect the lateral migration of GISTs cells. Meanwhile, longitudinal migration ability of cells was verified via the number of cells passing through uncoated Matrigel. In Fig. 6C, F, the longitudinal migration capacity of GIST-T1 and GIST-T1/IMR cells was similar ($P > 0.05$). After exposure to 20 μ M of IM for 48 h, the longitudinal migration capacity of both two cell lines decreased significantly ($P < 0.01$). Further, GIST-T1/IMR cells also exhibited higher longitudinal migration capacity than GIST-T1 cells ($P < 0.01$). Moreover, DMS could further block the ability of longitudinal migration of both two cell lines.

The invasiveness of cells within 48 h was detected by transwell chamber assay. The numbers of GIST-T1/IMR cells was lower than GIST-T1 cells ($P < 0.01$). Similarly significant differences were observed after IM intervention groups on both the GIST-T1 and GIST-T1/IMR cell line, when compared to control group. After DMS pretreatment and then IM treatment, the number of transmembrane cells was further reduced dramatically (Fig. 6D, G).

The colony formation ability of single cells in each group was tested by plate colony formation experiment. GIST-T1 and GIST-T1/IMR cells have similar colony formation ability. After IM intervention, the number of colony formation was significantly less than the control group ($P < 0.01$). Colony

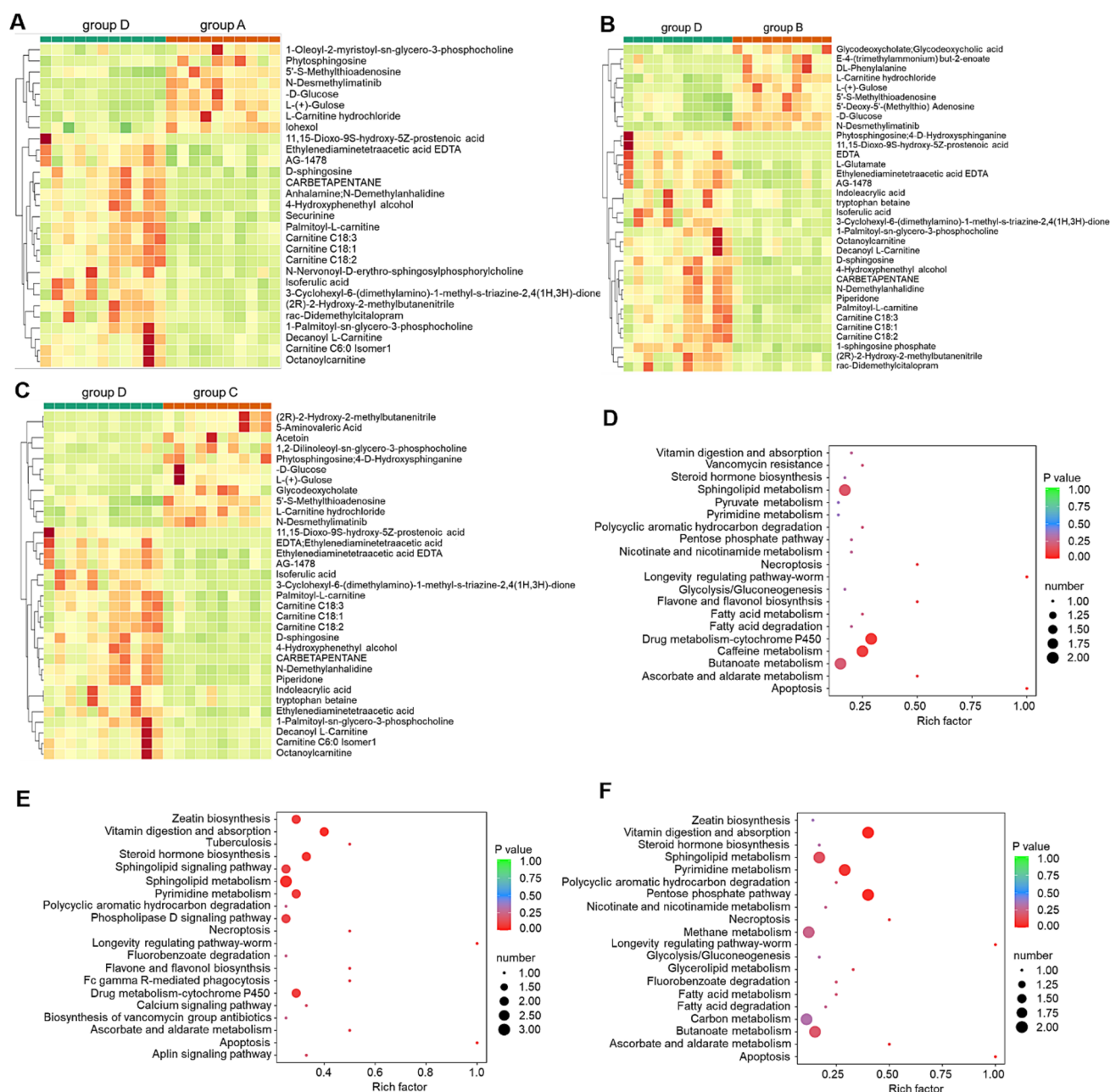


Fig. 5 Identification of potential metabolites and pathways. **A–C** The heat maps of the 20 differential metabolites from control group compared to treated group. **D–F** KEGG enrichment pathway impact analysis obtained from differential metabolites in group D compar-

son with group A to C. The color and size of each circle is based on *p* values (green: higher *p* values and red: lower *p* values) and pathway impact values (the larger the circle the higher the impact score) calculated from the topological analysis, respectively

formation ability was further reduced after DMS pretreatment, when compared with IM intervention's group ($P < 0.01$) (Fig. 6H, I).

The mechanism of SPK1/S1P pathway in IM-resistance

The inner function of SPK1/S1P axis on the GIST-T1 and GIST-T1/IMR cells were conducted in the cell cycle, cell

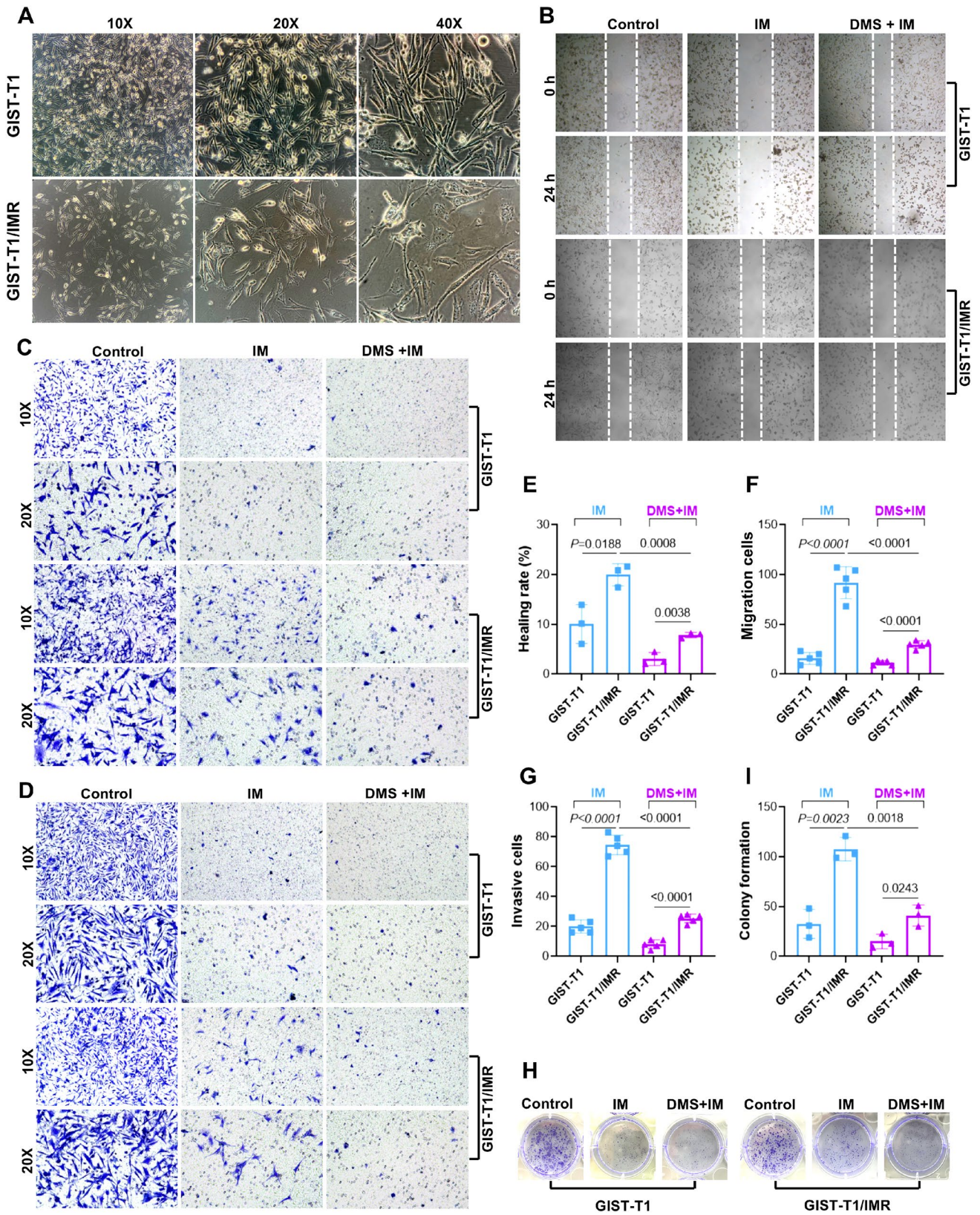


Fig. 6 Establishment of the IM-resistant GIST-T1/IMR cell line. **A** Cell morphology under microscope between GIST-T1 and GIST-T1/IMR cell line. **B, E.** Picture of lateral cell migration and scratch healing rate between GIST-T1 and GIST-T1/IMR cell line. **C, F** Picture

of longitudinal migration and migration rate between GIST-T1 and GIST-T1/IMR cell line. **D, G** Picture of cell transwell invasion and number of transmembrane cells. **H and I.** Picture of colony formation and formation rate

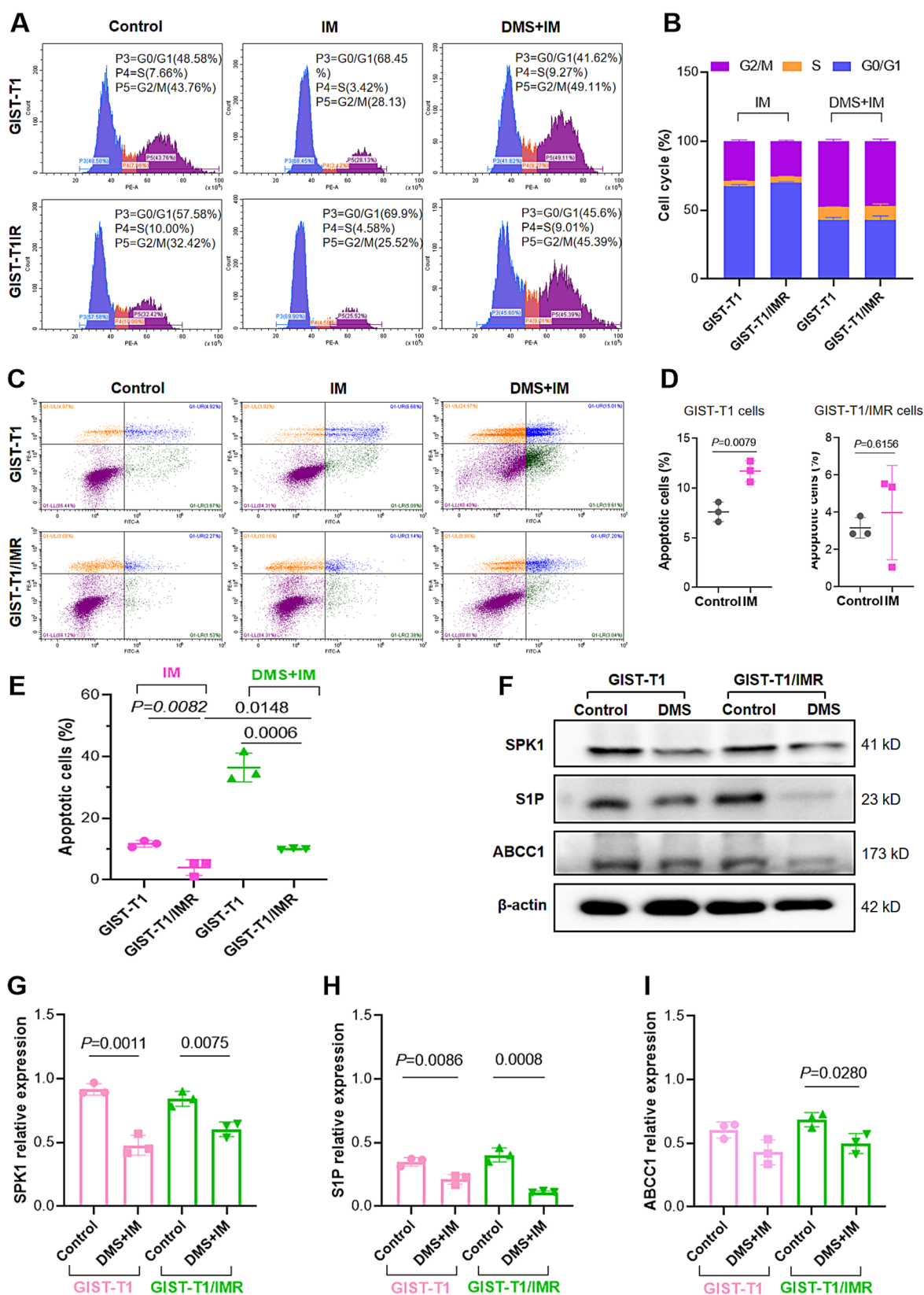


Fig. 7 The mechanism of SPK1/S1P pathway in IM-resistance cells. **A, B** The cell cycle of GIST-T1 and GIST-T1/IMR after the treatment of IM and DMS with IM. **C–E**. The cell apoptosis rate of GIST-

T1 and GIST-T1/IMR after the treatment of IM and DMS with IM, respectively. **F–I**. S1P, SPK1 and ABCC1 protein expression via western blot assay

apoptosis and protein expression studies.

As supplied by Fig. 7A, B, when exposed to IM ($P < 0.01$), a higher proportion of G0/G1 phase and a lower proportion of S and G2/M were appeared. The similar outcome was also arised on the GIST-T1/IMR cells. These findings suggested that IM could increase the proportion of G0/G1 phase to affect the growth activity of GIST-T1 and GIST-T1/IMR cell lines, respectively. After DMS interfered with SPK1/S1P signaling pathway, the proportion of G0/G1 phase on GIST-T1 and GIST-T1/IMR cells were significantly lower than that in only treatment with IM ($P < 0.01$), while the proportion of S and G2/M phase were increased correspondingly (Fig. 7B).

Cell apoptosis results (Fig. 7C–E) explained that the apoptosis rate of GIST-T1/IMR cells was similar to that of the parent cells ($P > 0.05$). And the apoptosis rate of GIST-T1 cells treated with IM alone was higher than that of the control group ($P < 0.01$). Further, the apoptosis rate of IM treatment group in GIST-T1 was higher than that of GIST-T1/IMR ($P < 0.05$), which verified that GIST-T1/IMR cells were less disturbed by IM. However, after DMS interference, the apoptosis rate were significantly higher than those of cells without DMS treatment, suggesting that DMS interference with SPK1/S1P signaling pathway could promote cell apoptosis, especially induce apoptosis of drug-resistant cell lines. Combined with the results of cell cycle and apoptosis, it suggested that DMS interference with SPK1/S1P could inhibit cell proliferation and promote apoptosis by blocking S and G2/M phases.

The specific protein expression was also investigated, as exhibited in Fig. 7F–I. ABCC1 is an important member of the ATP binding cassette (ABC) transporter family, which is central to mediate multidrug resistance (MDR) in naturally derived anticancer agents [64]. Herein, in this study, we also discussed the expression and function of ABCC1 on the IM-resistance cell line. The protein levels of S1P and ABCC1 proteins on the GIST-T1/IMR cells were up-regulated compared with those in the GIST-T1 cells, which further verified the successful construction of IM-resistant cell line. The protein levels of S1P, ABCC1 and SPK1 decreased after DMS blockage for 5 h, suggesting that interference with SPK1/S1P signaling pathway has the potential to reverse the occurrence of IM resistance.

Discussion

IM treatment for patients with GISTs is a lengthy process, and IM resistance is an obstacle for the further development of GISTs treatment. It is widely known that IM is a successful orally targeted drug that is metabolized by CYP450 [65]. Interpatient differences in pharmacokinetic (PK) variability have been estimated to be approximately 60%, as revealed by IM steady-state trough concentrations in patients with GISTs [66]. Based on our previous report [4], surgery, some

serum index and OCT1 SNP distribution have potential roles in disturbing the steady-state plasma concentration of IM.

One of the purposes of this study was to determine the key factors affecting the clinical efficacy of IM via the evaluation assay of TDM. After taken same dosage of IM, the patients with high and middle serum concentration of IM were considered as the sensitive IM treatment, while the patients with low serum concentration of IM (< 1100 ng/mL) were conducted as insensitivity to IM treatment. As above mentioned, the IM resistance would not be totally mimicked via serum concentration in clinic. If the patients were identified as IM-resistance type, they would be rapidly given second or third generation TKIs drugs. Herein, we conducted the plasma concentration as the core index to estimate the efficacy, which was convenience and operability in clinic. We found that the type of gastric surgery operation and body surface area were associated with IM steady-state concentration, in accordance with some reports [41, 42]. The OCT1 SNP distribution was assessed because OCT1 is considered to be the main influx transporter involved in IM uptake by chronic myelogenous leukaemia cells [67]. Lower OCT1 activity in diagnostic chronic myeloid leukaemia blood mononuclear cells is associated with a poorer molecular response to IM [28], and a molecular response to IM usually correlates with its plasma concentration [28]. Studies have also shown that drug resistance easily occurs when the effective blood drug concentration is low for a long time [68]. Because the actual role of OCT1 in GISTs is still unclear, we chose 5 SNPs of OCT1 for this study, and only 1386C > A (rs622342) showed a significant difference with regard to IM plasma concentration. This finding could be considered as preliminary for further research.

Through a series of metabolomics analyses, sphingolipid metabolism was selected as the most potential pathway in the treatment of IM. SPK1/S1P axis, the most important of the sphingolipid metabolism signal pathway involved with cancer, which could influence the direction of tumor progression [69]. Herein, we constructed the IM-resistance GIST cell line, GIST-T1/IMR, to simulate the IM-insensitive condition and explore the mechanism for IM resistance. The resistance index of GIST-T1/IMR constructed by IM induction was nearly 5, which met the criteria of resistance. The healing, migration, invasion and colony ability of GIST-T1/IMR cells were also stronger than GIST-T1 cells after treatment of IM. These data proved the IM-resistance cells exhibited lower sensibility of IM. After blockage the SPK1/S1P signal pathway with DMS, the migration, invasion and colony formation ability of cells in the GIST-T1 and GIST-T1/IMR groups were decreased, and the apoptotic rate was increased, respectively. With the help of DMS interference, the GIST-T1/IMR cells arrested in the S and G2/M phases, the sensitivity to IM was increased. The expression levels of S1P and

ABCC1 proteins in GIST-T1/IMR cells were significant higher than those in GIST-T1 cells, meanwhile the expression levels of S1P, SPK1 and ABCC1 protein in resistant cell lines were significantly down-regulated after DMS interference. Altogether, SPK1/S1P may participate the resistant process of GISTs to IM, indicated that inhibiting these signals may be benefit for IM long-term treatment.

Conclusion

IM-resistance is one of the challenges facing the treatment of advanced, unresectable/metastatic GISTs. In this study, the SNP of OCT1 1386C > A (rs 622342) is significantly related to the IM plasma concentration, but more samples are needed to confirm this result. The SPK1/S1P signaling pathway was first found out in the IM-treated GISTs from serum metabolites. Further, the role of SPK1/S1P axis was confirmed could confer the IM-sensitivity at the cellular level. Silencing SPK1/S1P signaling pathway could be a new promising approach to reverse IM-resistance.

Supplementary Information The online version contains supplementary material available at <https://doi.org/10.1007/s10120-022-01332-7>.

Acknowledgements The authors thank Prof. Wenbin Ou from Zhejiang Provincial Key Laboratory of Silkworm Bioreactor and Biomedicine, for kindly providing the valuable cell lines used in this study. This work was financially supported by the Outstanding Young Scientific Talent Foundation of Sichuan Province (No. 2022JDJQ0052); Science and Technology Program of Sichuan Province (No. 22NSFSC1458, No. 2022NSFSC0792, 2020YFS0417); Research Project of Sichuan Administration of Traditional Chinese Medicine (No. 2020JC0114); Beijing Xisike Clinical Oncology Research (No. Y-QL202101-0125); Technology Innovation Research and Development Project of Chengdu Science and Technology Bureau (No. 2021-YF05-02064-SN, No. 2022-YF05-01591-SN).

Author contributions YC conceived the study and wrote the paper; RZ collected the patients' samples and conducted the cell experiment. DDM and QJW constructed the plasma experiment. TWLH and XWD revised edition for the revising language, adjusting the framework, updating corresponding references; HWZ taken part in the care of the patients, especially in some adverse reaction; SJS and HTX aided in conceptualization and the supporting funding. The author(s) read and approved the final manuscript.

Availability of data and material All data generated or analysed during this study are included in this manuscript and its supplementary information files.

Declarations

Conflict of interest The authors declare that there are no conflicts of interest.

Ethics approval and consent to participate All participants provided informed consent to the protocol (Approval No. SCCHE-02–2020-

044) was approved by the Review Ethic Board at the Sichuan Cancer Hospital.

Consent for publication Not applicable.

References

1. Steeghs EMP, Gelderblom H, Ho VKY, Voorham QJM, Willemms SM, Grünberg K, Ligtenberg MJL, PATH consortium. Nationwide evaluation of mutation-tailored treatment of gastrointestinal stromal tumors in daily clinical practice. *Gastric Cancer*. 2021;24(5):990–1002. <https://doi.org/10.1007/s10120-021-01190-9>.
2. Zeng C, Zhu L, Jia X, Pang Y, Li Z, Lu X, Xie F, Duan L, Wang Y. Spectrum of activity of dasatinib against mutant KIT kinases associated with drug-sensitive and drug-resistant gastrointestinal stromal tumors. *Gastric Cancer*. 2020;23(5):837–47. <https://doi.org/10.1007/s10120-020-01069-1>.
3. Yoon H, Tang CM, Banerjee S, Yebra M, Noh S, Burgoyne AM, et al. Cancer-associated fibroblast secretion of PDGFC promotes gastrointestinal stromal tumor growth and metastasis. *Oncogene*. 2021;40:1957–73.
4. Chen Y, Dong X, Wang Q, Liu Z, Dong X, Shi S, et al. Factors influencing the steady-state plasma concentration of imatinib mesylate in patients with gastrointestinal stromal tumors and chronic myeloid leukemia. *Front Pharmacol*. 2020;11:569843.
5. Boichuk S, Galembikova A, Mikheeva E, Bikinieva F, Aukhadieva A, Dunaev P, et al. Inhibition of FGF2-mediated signaling in GIST-promising approach for overcoming resistance to imatinib. *Cancers (Basel)*. 2020;12:1674.
6. Proudman D, Miller A, Nellesen D, Gomes A, Mankoski R, Norregaard C, et al. Financial implications of avapritinib for treatment of unresectable gastrointestinal stromal tumors in patients with a PDGFRA Exon 18 variant or after 3 previous therapies in a hypothetical US health plan. *JAMA Netw Open*. 2020;3:e2025866.
7. Kelly CM, Gutierrez Sainz L, Chi P. The management of metastatic GIST: current standard and investigational therapeutics. *J Hematol Oncol*. 2021;14:2.
8. Narjuz C, Favre A, McMullen J, Kiehl P, Montemurro M, Figg WD, et al. Important role of CYP2J2 in protein kinase inhibitor degradation: a possible role in intratumor drug disposition and resistance. *PLoS ONE*. 2014;9:e95532.
9. Théou N, Gil S, Devocelle A, Julié C, Lavergne-Slove A, Beauchet A, et al. Multidrug resistance proteins in gastrointestinal stromal tumors: site-dependent expression and initial response to imatinib. *Clin Cancer Res*. 2005;11:7593–8.
10. Zhang Q, Li Z, Xu K, Qian Y, Chen M, Sun L, et al. Intracellular concentration and transporters in imatinib resistance of gastrointestinal stromal tumor. *Scand J Gastroenterol*. 2019;54:220–6.
11. Kumar V, Singh P, Gupta SK, Ali V, Verma M. Transport and metabolism of tyrosine kinase inhibitors associated with chronic myeloid leukemia therapy: a review. *Mol Cell Biochem*. 2022. <https://doi.org/10.1007/s11010-022-04376-6>.
12. Wang Q, Jiang ZP, Zeng J, Zhu Y, Cai HL, Xiang DX, et al. Effects of trough concentration and solute carrier polymorphisms on imatinib efficacy in Chinese patients with chronic myeloid leukemia. *J Pharm Pharm Sci*. 2020;2:1–9.
13. Flavahan WA, Drier Y, Johnstone SE, Hemming ML, Tarjan DR, Hegazi E, et al. Altered chromosomal topology drives oncogenic programs in SDH-deficient GISTs. *Nature*. 2019;575:229–33.
14. Llopis B, Robidou P, Tissot N, Pinna B, Gougis P, Aubart FC, et al. Development and clinical validation of a simple and fast

- UPLC-ESI-MS/MS method for simultaneous quantification of nine kinase inhibitors and two antiandrogen drugs in human plasma: Interest for their therapeutic drug monitoring. *J Pharm Biomed Anal.* 2021;197:113968.
15. Rutkowski P, Ziętek M, Cybulska-Stopa B, Streb J, Głuszek S, Jankowski M, et al. The analysis of 3-year adjuvant therapy with imatinib in patients with high-risk molecular profiled gastrointestinal stromal tumors (GIST) treated in routine practice. *Eur J Surg Oncol.* 2021;47:1191–5.
 16. Tartaglia S, Meneghello A, Bellotto O, Poetto AS, Zanchetta M, Posocco B, et al. An SPR investigation into the therapeutic drug monitoring of the anticancer drug imatinib with selective aptamers operating in human plasma. *Analyst.* 2021;146:1714–24.
 17. Grothey A, Blay JY, Pavlakis N, Yoshino T, Bruix J. Evolving role of regorafenib for the treatment of advanced cancers. *Cancer Treat Rev.* 2020;86:101993. <https://doi.org/10.1016/j.ctrv.2020.101993>.
 18. Elseud YA, Shaaban A, Mohanty A, Albarrak J. Safety and tolerability of regorafenib: a real-life experience. *J Gastrointest Cancer.* 2021. <https://doi.org/10.1007/s12029-020-00570-1>.
 19. Chang YR, Huang WK, Wang SY, Wu CE, Chen JS, Yeh CN. A nomogram predicting progression free survival in patients with gastrointestinal stromal tumor receiving sunitinib: incorporating pre-treatment and post-treatment parameters. *Cancers (Basel).* 2021;13(11):2587. <https://doi.org/10.3390/cancers13112587>.
 20. Lu X, Pang Y, Cao H, Liu X, Tu L, Shen Y, Jia X, Lee JC, Wang Y. Integrated screens identify CDK1 as a therapeutic target in advanced gastrointestinal stromal tumors. *Cancer Res.* 2021;81(9):2481–94. <https://doi.org/10.1158/0008-5472.CAN-20-3580>.
 21. Grunewald S, Klug LR, Mühlenberg T, Lategahn J, Falkenhorst J, Town A, Ehrh C, Wardelmann E, Hartmann W, Schildhaus HU, Treckmann J, Fletcher JA, Jung S, Czodrowski P, Miller S, Schmidt-Kittler O, Rauh D, Heinrich MC, Bauer S. Resistance to avapritinib in PDGFRA-driven GIST is caused by secondary mutations in the PDGFRA kinase domain. *Cancer Discov.* 2021;11(1):108–25. <https://doi.org/10.1158/2159-8290.CD-20-0487>.
 22. Blay JY, Serrano C, Heinrich MC, Zalcberg J, Bauer S, Gelderblom H, Schöffski P, Jones RL, Attia S, D'Amato G, Chi P, Reichardt P, Meade J, Shi K, Ruiz-Soto R, George S, von Mehren M. Ripretinib in patients with advanced gastrointestinal stromal tumours (INVICTUS): a double-blind, randomised, placebo-controlled, phase 3 trial. *Lancet Oncol.* 2020;21(7):923–34. [https://doi.org/10.1016/S1470-2045\(20\)30168-6](https://doi.org/10.1016/S1470-2045(20)30168-6).
 23. Carriot N, Paix B, Greff S, Viguier B, Briand JF, Culioli G. Integration of LC/MS-based molecular networking and classical phytochemical approach allows in-depth annotation of the metabolome of non-model organisms—the case study of the brown seaweed *Taonia atomaria*. *Talanta.* 2021;225:121925.
 24. Nigam SK. The SLC22 transporter family: a paradigm for the impact of drug transporters on metabolic pathways, signaling, and disease. *Annu Rev Pharmacol Toxicol.* 2018;6(58):663–87. <https://doi.org/10.1146/annurev-pharmtox-010617-052713>.
 25. Brosseau N, Ramotar D. The human organic cation transporter OCT1 and its role as a target for drug responses. *Drug Metab Rev.* 2019;51:389–407.
 26. Morse BL, Kolar A, Hudson LR, Hogan AT, Chen LH, Brackman RM, et al. Pharmacokinetics of organic cation transporter 1 (OCT1) substrates in Oct1/2 knockout mice and species difference in hepatic OCT1-mediated uptake. *Drug Metab Dispos.* 2020;48:93–105.
 27. Chang HH, Hsueh YS, Cheng YW, Ou HT, Wu MH. Association between polymorphisms of OCT1 and metabolic response to metformin in women with polycystic ovary syndrome. *Int J Mol Sci.* 2019;20:1720.
 28. Wang J, Lu L, Kok CH, Saunders VA, Goyne JM, Dang P, Leclercq TM, Hughes TP, White DL. Increased peroxisome proliferator-activated receptor γ activity reduces imatinib uptake and efficacy in chronic myeloid leukemia mononuclear cells. *Haematologica.* 2017;102(5):843–53. <https://doi.org/10.3324/haematol.2016.153270>.
 29. Xinwei D, Gang J, Songtao M, Yan C. Simultaneous determine of imatinib mesylate and its metabolites in human plasma by two-dimensional liquid chromatography: a methodological study. *J Cancer Control Treat.* 2021;34(10):919–26.
 30. Wang Q, Jiang ZP, Zeng J, Zhu Y, Cai HL, Xiang DX, et al. Effects of trough concentration and solute carrier polymorphisms on imatinib efficacy in chinese patients with chronic myeloid leukemia. *J Pharm Pharm Sci.* 2020;23:1–9.
 31. Chen W, Kuang Y, Qiu HB, Cao Z, Tu Y, Sheng Q, Eilers G, He Q, Li HL, Zhu M, Wang Y, Zhang R, Wu Y, Meng F, Fletcher JA, Ou WB. Dual targeting of insulin receptor and KIT in imatinib-resistant gastrointestinal stromal tumors. *Cancer Res.* 2017;77(18):5107–17. <https://doi.org/10.1158/0008-5472.CAN-17-0917>.
 32. Zhou Y, Chen J, Weng X, Lin G, Huang Z, Shui H. Establishment of a GIST-T1 gastrointestinal stromal tumour cell line resistant to imatinib mesylate. *Oncol Lett.* 2018;15(5):7589–94. <https://doi.org/10.3892/ol.2018.8283>.
 33. Chen K, Ren Q, Han XR, Zhang XN, Wei B, Bai XZ. Imatinib mesylate induces mitochondria-dependent apoptosis and inhibits invasion of human pigmented villonodular synovitis fibroblast-like synovial cells. *Oncol Rep.* 2016;35(1):197–204. <https://doi.org/10.3892/or.2015.4350>.
 34. Su B, Huang T, Jin Y, Yin H, Qiu H, Yuan X. Apatinib exhibits synergistic effect with pyrotinib and reverses acquired pyrotinib resistance in HER2-positive gastric cancer via stem cell factor/c-kit signaling and its downstream pathways. *Gastric Cancer.* 2021;24(2):352–67. <https://doi.org/10.1007/s10120-020-01126-9>.
 35. Vetter TR. Fundamentals of research data and variables: the devil is in the details. *Anesth Analg.* 2017;125:1375–80.
 36. Vermeulen K, Thas O, Vansteelandt S. Increasing the power of the Mann–Whitney test in randomized experiments through flexible covariate adjustment. *Stat Med.* 2015;34:1012–30.
 37. Mishra P, Singh U, Pandey CM, Mishra P, Pandey G. Application of student's *t*-test, analysis of variance, and covariance. *Ann Card Anaesth.* 2019;22:407–11.
 38. Belsey SL, Ireland R, Lang K, Kizilors A, Ho A, Mufti GJ, et al. Women administered standard dose imatinib for chronic myeloid leukemia have higher dose-adjusted plasma imatinib and norimatinib concentrations than men. *Ther Drug Monit.* 2017;39:499–504.
 39. Gotta V, Bouchet S, Widmer N, Schuld P, Decosterd LA, Buclin T, et al. Large-scale imatinib dose-concentration-effect study in CML patients under routine care conditions. *Leuk Res.* 2014;38:764–72.
 40. Chen Y, Shen T, Zhong L, Liu Z, Dong X, Huang T, et al. Research progress of chloroquine and hydroxychloroquine on the COVID-19 and their potential risks in clinic use. *Front Pharmacol.* 2020;11:1167.
 41. Yoo C, Ryu MH, Kang BW, Yoon SK, Ryoo BY, Chang HM, et al. Cross-sectional study of imatinib plasma trough levels in patients with advanced gastrointestinal stromal tumors: impact of gastrointestinal resection on exposure to imatinib. *J Clin Oncol.* 2010;28:1554–9.
 42. Hompland I, Bruland ØS, Ubhayasekhara K, Bergquist J, Boye K. Clinical implications of repeated drug monitoring of imatinib in patients with metastatic gastrointestinal stromal tumour. *Clin Sarcoma Res.* 2016;6:21.
 43. Peng B, Lloyd P, Schran H. Clinical pharmacokinetics of imatinib. *Clin Pharmacokinet.* 2005;44(9):879–94.

44. Demetri GD, Wang Y, Wehrle E, Racine A, Nikolova Z, Blanke CD, et al. Imatinib plasma levels are correlated with clinical benefit in patients with unresectable/metastatic gastrointestinal stromal tumors. *J Clin Oncol*. 2009;27:3141–7.
45. Vaidya S, Ghosh K, Shanmukhaiah C, Vundinti BR. Genetic variations of hOCT1 gene and CYP3A4/A5 genes and their association with imatinib response in Chronic Myeloid Leukemia. *Eur J Pharmacol*. 2015;765:124–30.
46. Sánchez-Illana Á, Piñeiro-Ramos JD, Sanjuan-Herráez JD, Vento M, Quintás G, Kuligowski J. Evaluation of batch effect elimination using quality control replicates in LC-MS metabolite profiling. *Anal Chim Acta*. 2018;1019:38–48.
47. Li H, Zhu Q, Li K, Wu Z, Tang Z, Wang Z. Investigation of urinary components in rat model of ketamine-induced bladder fibrosis based on metabolomics. *Transl Androl Urol*. 2021;10:830–40.
48. Zhang R, Ross AB, Yoo MJY, Farouk MM. Metabolic fingerprinting of in-bag dry- and wet-aged lamb with rapid evaporative ionisation mass spectroscopy. *Food Chem*. 2021;347:128999.
49. Tuy-On T, Itharat A, Maki P, Thongdeeying P, Pipatattanaseree W, Ooraiikul B. In vitro cytotoxic activity against breast, cervical, and ovarian cancer cells and flavonoid content of plant ingredients used in a selected thai traditional cancer remedy: correlation and hierarchical cluster analysis. *Evid Based Complement Alternat Med*. 2020;2020:8884529.
50. Du Y, Fan P, Zou L, Jiang Y, Gu X, Yu J, et al. Serum metabolomics study of papillary thyroid carcinoma based on HPLC-Q-TOF-MS/MS. *Front Cell Dev Biol*. 2021;9:593510.
51. Gong H, Wang X, Liu B, Boutet S, Holcomb I, Dakshinamoorthy G, et al. Single-cell protein-mRNA correlation analysis enabled by multiplexed dual-analyte co-detection. *Sci Rep*. 2017;7:2776.
52. Kanehisa M, Furumichi M, Tanabe M, Sato Y, Morishima K. KEGG: new perspectives on genomes, pathways, diseases and drugs. *Nucleic Acids Res*. 2017;45:D353–61.
53. Abooshahab R, Hooshmand K, Razavi SA, Gholami M, Sanoie M, Hedayati M. Plasma metabolic profiling of human thyroid nodules by gas chromatography-mass spectrometry (GC-MS)-based untargeted metabolomics. *Front Cell Dev Biol*. 2020;8:385.
54. Ogretmen B. Sphingolipid metabolism in cancer signalling and therapy. *Nat Rev Cancer*. 2018;18:33–50.
55. Olson KC, Moosic KB, Jones MK, Larkin PMK, Olson TL, Toro MF, et al. Large granular lymphocyte leukemia serum and corresponding hematological parameters reveal unique cytokine and sphingolipid biomarkers and associations with STAT3 mutations. *Cancer Med*. 2020;9:6533–49.
56. Xu R, Antwi Boasiako P, Mao C. Alkaline ceramidase family: the first two decades. *Cell Signal*. 2021;78:109860.
57. Roy S, Khan S, Jairajpuri DS, Hussain A, Alajmi MF, Islam A, et al. Investigation of sphingosine kinase 1 inhibitory potential of cinchonine and colcemid targeting anticancer therapy. *J Biomol Struct Dyn*. 2021;10:1–13. <https://doi.org/10.1080/07391102.2021.1882341>.
58. Hii LW, Chung FF, Mai CW, Yee ZY, Chan HH, Raja VJ, et al. Sphingosine kinase 1 regulates the survival of breast cancer stem cells and non-stem breast cancer cells by suppression of STAT1. *Cells*. 2020;9:886.
59. Liu L, Zhou XY, Zhang JQ, Wang GG, He J, Chen YY, et al. LncRNA HULC promotes non-small cell lung cancer cell proliferation and inhibits the apoptosis by up-regulating sphingosine kinase 1 (SPHK1) and its downstream PI3K/Akt pathway. *Eur Rev Med Pharmacol Sci*. 2018;22(24):8722–30. https://doi.org/10.26355/eurrev_201812_16637.
60. Li QF, Yan J, Zhang K, Yang YF, Xiao FJ, Wu CT, et al. Bortezomib and sphingosine kinase inhibitor interact synergistically to induces apoptosis in BCR/ABI+ cells sensitive and resistant to STI571 through down-regulation Mcl-1. *Biochem Biophys Res Commun*. 2011;405:31–6.
61. Xu X, Yin S, Ren Y, Hu C, Zhang A, Lin Y. Proteomics analysis reveals the correlation of programmed ROS-autophagy loop and dysregulated G1/S checkpoint with imatinib resistance in chronic myeloid leukemia cells. *Proteomics*. 2022;22(1–2):e2100094. <https://doi.org/10.1002/pmic.202100094>.
62. Escudero-Casao M, Cardona A, Beltrán-Debón R, Díaz Y, Matheu MI, Castellón S. Fluorinated triazole-containing sphingosine analogues. Syntheses and in vitro evaluation as SPHK inhibitors. *Org Biomol Chem*. 2018;16(39):7230–5. <https://doi.org/10.1039/c8ob01867g>.
63. Huang M, Yang W, Zhu J, Mariño-Enríquez A, Zhu C, Chen J, Wu Y, Quan Y, Qiu H, Li X, Chai L, Fletcher JA, Ou WB. Coordinated targeting of CK2 and KIT in gastrointestinal stromal tumours. *Br J Cancer*. 2020;122(3):372–81. <https://doi.org/10.1038/s41416-019-0657-5>.
64. Chen XY, Yang Y, Wang JQ, Wu ZX, Li J, Chen ZS. Overexpression of ABCC1 confers drug resistance to betulin. *Front Oncol*. 2021;25(11):640656. <https://doi.org/10.3389/fonc.2021.640656>.
65. Pena MÁ, Muriel J, Saiz-Rodríguez M, Borobia AM, Abad-Santos F, Frías J, et al. Effect of cytochrome P450 and ABCB1 polymorphisms on Imatinib pharmacokinetics after single-dose administration to healthy subjects. *Clin Drug Investig*. 2020;40:617–28.
66. Gandia P, Arellano C, Lafont T, Huguet F, Malard L, Chatelut E. Should therapeutic drug monitoring of the unbound fraction of imatinib and its main active metabolite *N*-desmethyl-imatinib be developed? *Cancer Chemother Pharmacol*. 2013;71:531–6.
67. Chhikara S, Sazawal S, Seth T, Chaubey R, Singh K, Sharma R, et al. Molecular response to imatinib and its correlation with mRNA expression levels of imatinib influx transporter (OCT1) in Indian chronic myeloid leukemia patients. *Asian Pac J Cancer Prev*. 2017;18(8):2043–8. <https://doi.org/10.22034/APJCP.2017.18.8.2043>.
68. Vasan N, Baselga J, Hyman DM. A view on drug resistance in cancer. *Nature*. 2019;575:299–309.
69. Park WJ, Song JH, Kim GT, Park TS. Ceramide and sphingosine 1-phosphate in liver diseases. *Mol Cells*. 2020;43(5):419–30. <https://doi.org/10.14348/molcells.2020.0054>.

Publisher's Note Springer Nature remains neutral with regard to jurisdictional claims in published maps and institutional affiliations.

Springer Nature or its licensor holds exclusive rights to this article under a publishing agreement with the author(s) or other rightsholder(s); author self-archiving of the accepted manuscript version of this article is solely governed by the terms of such publishing agreement and applicable law.